IRRADIATION DAMAGE STUDIES IN SOLID TARGETS*

N. Simos#, H. Kirk, J. O Conor, L. Mausner, BNL, Upton, NY 11973, U.S.A.
K. McDonald, Princeton University, Princeton, NJ 08544, U.S.A.
N. Mokhov, FNAL, Batavia, IL 60510, U.S.A.

Abstract

In an effort to address the limitations on high-power accelerator target performance prompted by the elevated dose levels and the associated irradiation damage, an experimental study has been conducted to explore interesting new alloys and composites under the influence of protons and neutrons. Material irradiations were performed using the 200-MeV protons of the BNL Linac operating with an effective power of 18 kW. Selective results of the post-irradiation analysis of composites and "super" alloys depicting the effects on their physical and mechanical properties are presented. The post-irradiation analysis reveals interesting damage reversal by some of the promising candidate materials and unexpected low threshold of radiation resistance by others. Also included is a discussion of the correlation between proton- and neutron-induced damage and of the associated experimental effort to unravel such correlations.

INTRODUCTION

Multi-MW, high-performance proton beam targets are the key toward the next generation of accelerator machines such as those producing intense muon or neutrino beams. In pursuit of this goal one must push the envelope of the current knowledge of material science, material endurance, and survivability to both short and long proton beam exposure. The demand imposed on the targets of high-power accelerators and the limitations of most materials in playing such pivotal roles have led to an extensive search and experimentation with new alloys and composites. These new high-performance materials, developed to support technologies unrelated to accelerators and their targets, but which at first glance appear to possess the right combination of mechanical and physical properties, are explored through a multi-phased experimental study at Brookhaven National Laboratory (BNL). The overall study, which brings together the interest in accelerator targets of different facilities and accelerator initiatives from around the world (*i.e.,* neutrino factory/muon collider, neutrino superbeams, etc.), seeks to simulate conditions of both short and long exposure to proton beams and assess the survivability potential of solid materials. Figure 1 depicts a high-power target concept for a proposed multi-MW neutrino super-beam experiment. The concept shown is built around the anticipated performance of the low-*Z* carbon-carbon composite that constitutes the muon production target. This carbon composite, at the time of the study, appeared to possess the right combination of physio-mechanical properties that would enable it to function and meet the performance criteria of the high power accelerator. Performance and survivability in a multi-MW setting of a target represents the limiting factor. Performance is controlled by the ability of the target material to maintain key properties, such as density, and thus maintain the production of the secondary particles. Survivability in such environment is linked to both short- and long-term exposures. During short exposure the effect of the thermo-mechanical shock on the solid target of choice is the governing parameter, and therefore the limits of pulse intensity that can be tolerated needs to be established. To address the target-shock problem, experiments were conducted in the recent past using high-intensity proton pulses from the BNL AGS at 24 GeV on various solid targets. Experimental results revealed (a) the superiority of composites such as carbon-carbon over graphite to absorb shock, and (b) that advancements in computational science and simulation have matured enough to allow the exploration of solid-target response to yet-to-be-achieved intense pulses.

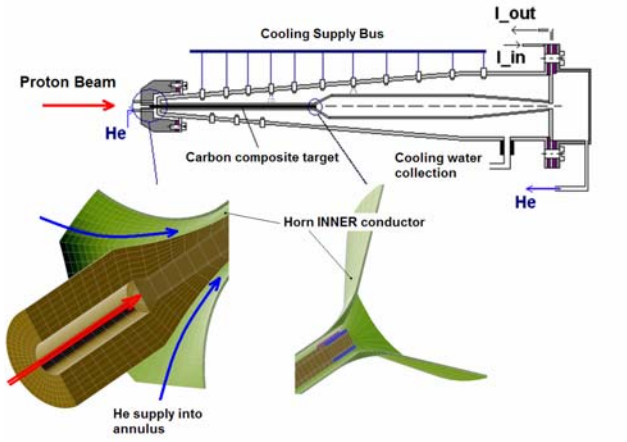

Figure 1: Target concept for a neutrino super-beam.

The effects of prolonged radiation exposure in composites and alloys that appear to be suitable have been under study through an extensive experimental program built around the high proton fluences of the BNL Linac beam serving the BNL Isotope Production Facility [1,2, 3]. The BNL Linac provides 200- or 117-MeV protons on irradiation targets with an integrated current of 85-90 μA. Special arrangement of the target layout during the latest irradiation phase has enabled the exposure of target materials primarily to neutron and gamma fluxes. While post-irradiation analysis of these exposures is pending, the details of this effort are discussed in this paper because of

*Work supported by the US DOE
#simos@bnl.gov

the importance of comparing the effects of protons with those of neutrons on material properties.

Presented in this paper are results of the post-irradiation analysis seeking to assess the changes taking place in mechanical and physical properties of different composites and super alloys. Irradiation levels in terms of displacements per atom (dpa) expected to trigger or reveal changes occurring in the material structure have been achieved in the course of the experimental study. Post-irradiation analysis results depicting changes in key physical properties such as thermal expansion and conductivity, including annealing and damage reversal as well as degradation of mechanical properties, such as loss of ductility, are presented and discussed. Results depicting the vulnerability of carbon-based materials (either in the form of graphite or composites) to high proton fluxes are examined while attempting to correlate the effects of energetic protons to neutrons. Also examined and presented are the effects of irradiation on various super-alloys such as super-Invar and "gum" metal.

IRRADIATION EXPERIMENT

Shown in Fig. 2 is the BNL accelerator where irradiation of the target materials is conducted. Specifically, the proton beam at the end of the Linac (at either 200- or 117-MeV energies) is directed toward the BLIP target station and onto the target assemblies. The layout of the matrix of materials being irradiated is depicted in Fig. 3. The incoming proton beam is degraded as it irradiates the multitude of layers. Listed in the array are the various alloys and composites irradiated during one of the exposures. The plan view represents the actual formation of one of the layers which consists of tensile specimens ("dog-bones") and specimens specially designed to evaluate thermal expansion and conductivity. Thin nickel foils placed within the irradiated layers and their subsequent radiography provided the necessary information to reconstruct the beam profile and distribution of dose within each specimen. Shown in Fig. 3 are special channels that allowed for cooling water to flow past the specimens and control the irradiation temperature.

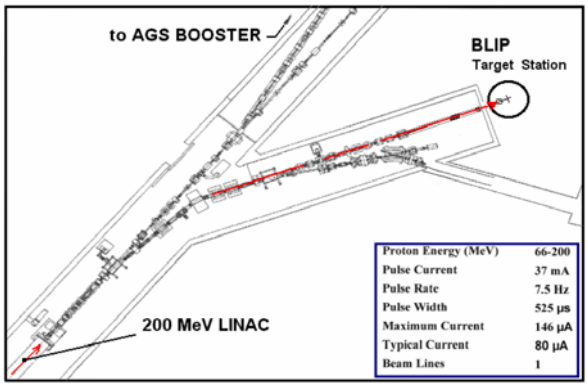

Figure 2: Layout of proton irradiating beam at BNL.

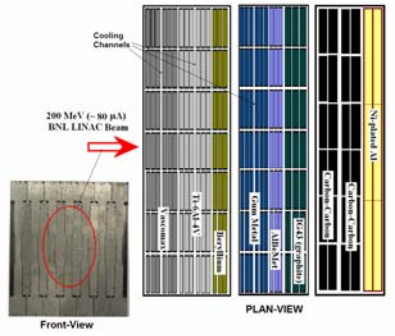

Figure 3: Layout of proton irradiating beam at BNL.

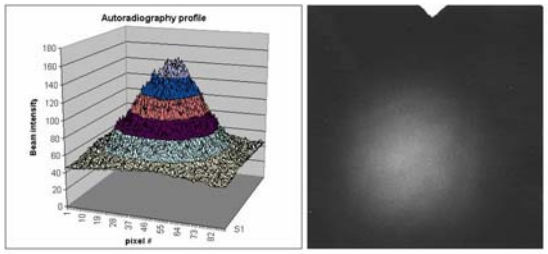

Figure 4: Beam profile and autoradiography.

Given that irradiation induced changes in materials have been primarily studied in nuclear reactors, and our studies are mainly with proton beams, we desired to establish the correlation between the effects of irradiation by protons and neutrons under similar conditions. A special set-up at the BNL BLIP target station created a "neutron" that exposed the target materials primarily to neutrons and gamma rays. Figure 5 depicts the arrangement by which neutron irradiation was achieved. Specifically, an array of isotope-production targets situated upstream of the accelerator target assembly are responsible for stopping the incoming primary protons (confirmed by MARS [8] calculations as shown in Fig. 5) while generating a flux downstream consisting of primarily of neutrons and gammas. Figure 6 shows the calculated neutron and gamma spectra in one of the accelerator target layers downstream of the stopped primary proton location.

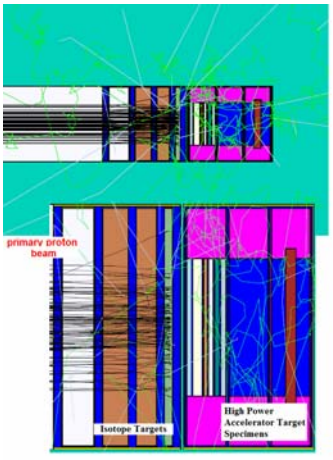

Figure 5: Layout of proton irradiating beam at BNL.

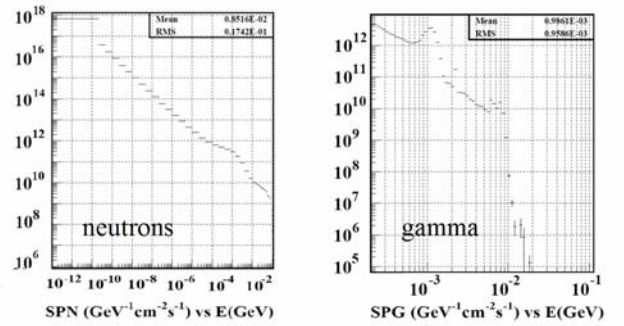

Figure 6: Calculated neutron and gamma energy spectra.

POST-IRRADIATION ANALYSIS

Carbon Composites and Graphite

In order to assess the validity of the high-power accelerator target concept of Fig.1, representing a pion production and capture concept for a multi-MW neutrino superbeam, attention was focused on carbon-based materials such as carbon composites and graphite. Experiments conducted at BNL [4] with a 24 GeV intense beam on target (~4.0 x10^{12} protons/pulse and 0.5-mm rms beam spot) have demonstrated the excellent shock resistance of carbon composites due to their extremely low thermal expansion coefficient. Aided by its high thermal conductivity, as compared to graphite, the carbon composite was selected as the target material for the neutrino superbeam study. The limited information available, however, on its resistance to prolonged radiation exposure prompted a series of irradiation studies. In these studies, which achieved peak proton fluences between 2x10^{20} – 1x10^{21} protons/cm^2, 2-D and 3-D weave carbon composites were exposed, as well as fine-grained graphite types such as IG-43 and IG-430. In addition, a special graphite-to-titanium bond was also irradiated to assess its vulnerability to high irradiation dose.

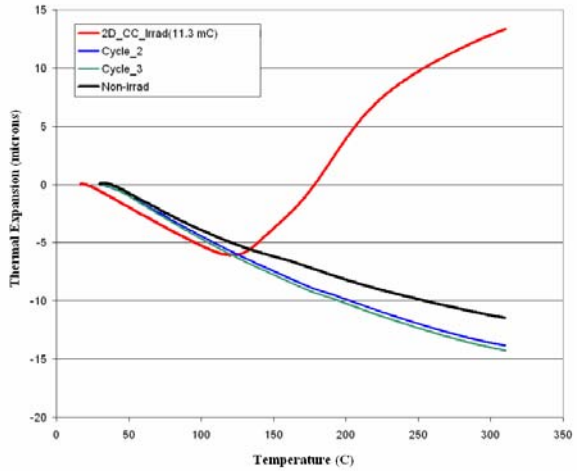

Figure 7: Post-irradiation thermal annealing of 2-D type carbon composite (fiber plane).

Post-irradiation analysis of carbon composites and graphite following exposure to proton fluences < 5x10^{20} p/cm^2 revealed some very interesting behavior. In particular, both carbon composite types (2-D and 3-D) experienced dramatic change in their thermal expansion coefficient, as shown in Figures 7-9. Figures 7 and 8 represent thermal expansion in the strong direction (along the reinforcing fibers). Figure 9 shows the effect of different dose levels (expressed in Curies) on the thermal expansion in a 2-D type carbon composite in the weak direction (normal to the fibers). In all cases, however, the composite exhibited the remarkable ability to reverse the "damage" through thermal annealing. This constitutes a very important feature in that the target material, if operated at high enough temperature, can reverse the degradation of the thermal expansion while damage is induced by the irradiation.

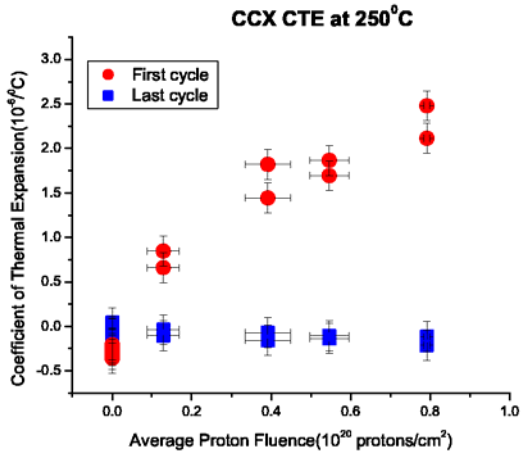

Figure 8: Recovery of thermal expansion coefficient of a 3-D type carbon composite following irradiation.

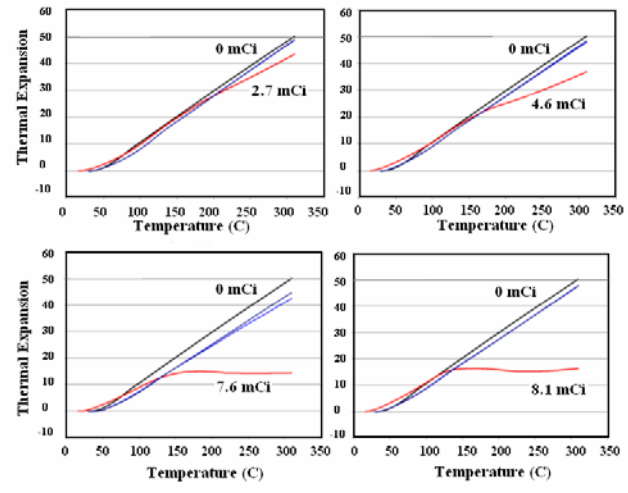

Figure 9: Thermal annealing of a 2-D type carbon composite along the direction normal to the fibers.

Figure 10 shows the influence of irradiation dose on the thermal expansion coefficient of the IG-43 graphite. Clearly, this graphite does not experience the dramatic changes observed in carbon composite with the onset of

irradiation (it only experiences a slight increase in the already much higher coefficient), but it also did not exhibit, at least for the annealing temperatures (up to 300 ^{o}C), reversal of the effect induced by irradiation.

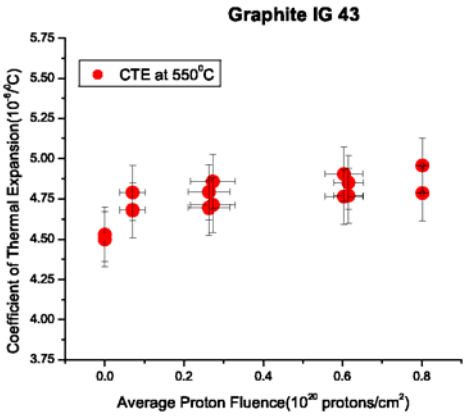

Figure 10: Effect of proton fluence on the coefficient of thermal expansion in IG-43 graphite.

Increased proton fluence levels (~10^{21} p/cm^2) achieved during two independent phases of the irradiation study have shown that both carbon composite types are susceptible to irradiation. Structural degradation was observed (Fig. 11) when fluences crossed the threshold 5x10^{20} p/cm^2. The results were reproduced in a follow-up study that reached similar dose levels. Most surprising, however, was the susceptibility of the IG-43 graphite (Fig. 11). In thermal-neutron irradiation studies elsewhere, graphite has sustained irradiation damage of several dpa without signs of structural degradation. In our studies with energetic protons, the dpa level in the damaged zone is estimated to be close to one. Further discussion of this discrepancy is included in the summary section.

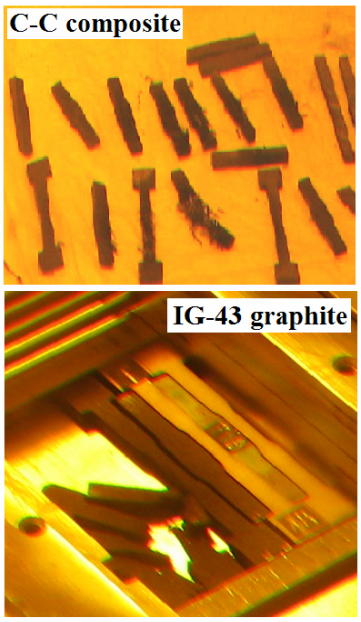

Figure 11: Damage induced by high proton fluences (~10^{21} protons/cm^2) on graphite and carbon composites.

Figure 12 depicts the pre-irradiated bond between graphite and titanium as viewed with a SEM, and the post-irradiated state (fluence of 10^{21} p/cm^2) which exhibits the same structural degradation seen in the graphite matrix (Fig. 11). The presence of water and its potential absorption by the graphite leading to galvanic corrosion has been considered as a contributing factor. However, the irradiation temperature has been estimated to be below the oxidation temperature of graphite.

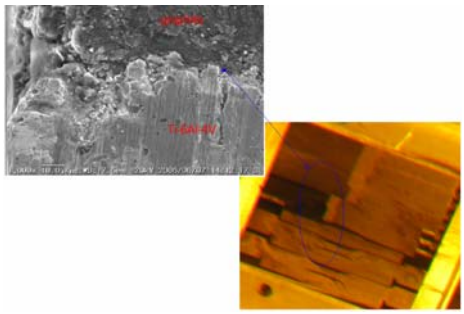

Figure 12: Microscopic view of a special graphite-to-titanium bond (left), and the effects of irradiation (right).

High thermal conductivity is a desirable physical property of materials destined for high-power accelerator targets. Neutron irradiation studies [5] have shown (Fig 13) that fine-grained isotropic graphite and carbon composites experience a dramatic reduction in thermal conductivity. Thermal annealing at elevated temperatures helps restore some of the lost conductivity. Thermal conductivity measurements, following proton irradiation, were made on graphite and carbon composites as part of this experimental study, with preliminary observation of a dramatic decrease in conductivity, as in the case of neutron irradiation. The reduction factor associated with ~0.25 dpa of proton irradiation in the carbon composite is 4 for both 2-D and 3-D types and 6 for the IG-43 graphite. The trend is quite similar with that of the data shown in Fig. 13 of neutron irradiation under similar temperature.

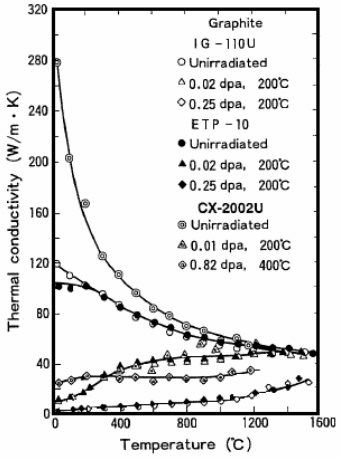

Figure 13: Effects of neutron irradiation on thermal conductivity of graphite and carbon composites [5].

Irradiation Effects on Super-alloys

A number of alloys exhibiting physio-mechanical properties desirable in high-power accelerator targets have been developed. Typically, low thermal expansion, high conductivity, low elasticity modulus, high ductility and fatigue resistance are some of the properties or combinations of that are desired. Certain materials known as super-alloys appear, at least in their un-irradiated state, as serious candidates. These include alloys such as super-Invar which exhibits very low thermal expansion in the range of 0-150°C, the titanium alloy Ti-6Al-4V, Vascomax, and the "gum" metal (Ti-12Ta-9Nb-3V-6Zr-O) [6] with "super" properties such as ultra-low elastic modulus, ultra-high strength, super plasticity and ultra-low expansion (invar-like behavior expanded to 400°C). These properties attributed to "gum" metal are linked to dislocation-free plastic deformations mechanisms associated with elastic strain fields that range from nanometer scale to several tens of micrometers. The effect of prolonged irradiation, however, on the properties of these materials has yet to be understood due to limited use in radiation environments. This experimental study is an attempt to fill some of the knowledge gaps by utilizing experience in other alloys that have been used extensively in both reactor and accelerator technologies.

Shown in Fig. 14 is the removal of neutron-induced defects in 304-type stainless steel [7] through thermal annealing. Such damage reversal has been already discussed as it pertains to carbon composites. The relevance, however, of these data is demonstrated in Figures 15 and 16 where complete reversal of irradiation-induced damage in super-invar is achieved through annealing. Super-invar was irradiated to a damage level of 0.25 dpa and its thermal expansion property was analyzed. It was found that the material had lost its characteristic, low expansion even at this moderate damage level. Given that the alloy is primarily iron, it was subjected to thermal cycling until the temperature threshold of 600°C was established where a complete reversal occurs. This is different from the behavior of typical metals like the one shown in Fig. 14 for which re-irradiation introduces a greater number of defects that are difficult to anneal.

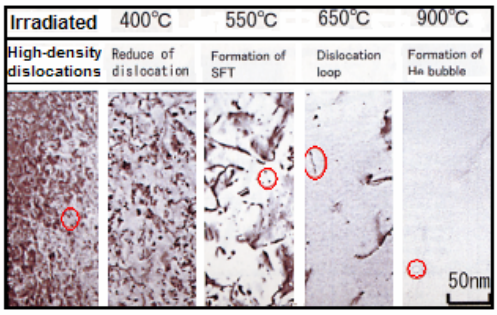

Figure 14: Annealing effects following neutron irradiation of type-304 stainless steel [7].

Figure 16 depicts the reversal of damage in super-invar following annealing of the first irradiation and re-exposure to about 1 dpa of damage. Apparently the material is able to "spring-back" to its undamaged state. To explore this particular behavior further, the twice-irradiated and annealed material has been exposed to a neutron flux with the set-up discussed earlier in the paper. Results of the post-irradiation analysis are still pending.

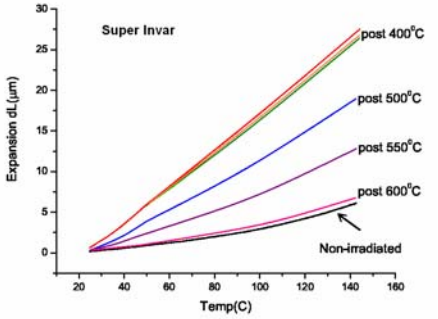

Figure 15: Annealing of super-Invar following proton irradiation to ~0.25 dpa.

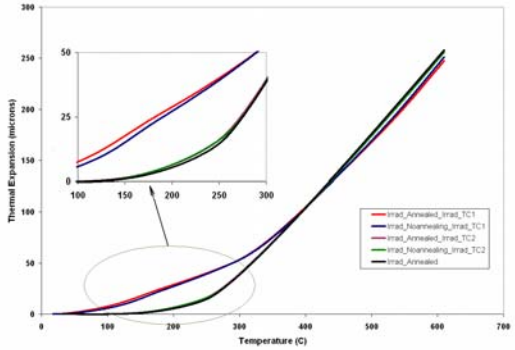

Figure 16: Damage reversal in super-Invar following annealing and re-irradiation.

Shown in Fig. 17 is the dependence of the thermal expansion coefficient of Ti-6Al-4V on proton fluence, and the stress-strain relationship at different levels of dpa damage. As indicated, the thermal expansion property of the alloy is increased minimally with increased fluence. The effect on the mechanical behavior is quite typical with what has been observed in metals irradiated with neutrons, *i.e.,* increase in strength accompanied by reduction in ductility.

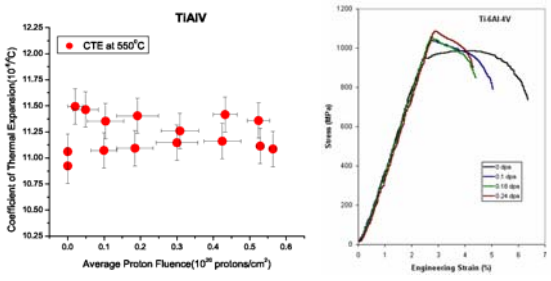

Figure 17: Irradiation effects on thermal expansion and the stress-strain relation of Ti-6Al-4V.

The experimental study explored the irradiated behavior of Vascomax, one the strongest steel alloys available. Figure 18 depicts the relationship between damage and thermal expansion as well as stress-strain. Similar to the case of Ti-6Al-4V, the effect on thermal expansion is minimal. What is important, however, is that the material gets stronger with irradiation while maintaining its ductility. Post-irradiation analysis of both Vascomax and Ti-6Al-4V at 1 dpa level damage achieved during the most recent irradiation is still pending.

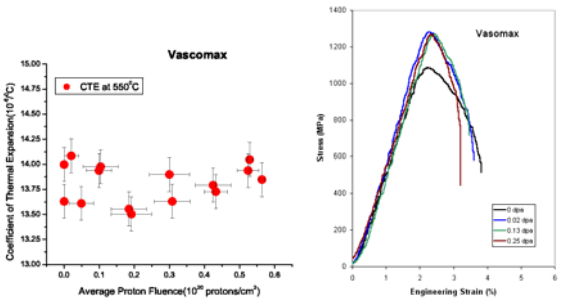

Figure 18: Irradiation effects on thermal expansion and stress-strain relationship of Vascomax.

The post-irradiation analysis of the super-alloy gum metal revealed that the material is extremely sensitive to irradiation as well as temperature. As indicated in Fig. 19, modest levels of proton damage (~0.25 dpa) are enough to remove the super-ductility of the alloy in its entirety. The analysis also revealed that the invar-like behavior of the gum metal (low thermal expansion) is affected less by irradiation than by a single thermal cycle which crosses the threshold temperature of ~550°C representing the of the phase transformation in the material microstructure (as seen in Fig. 19).

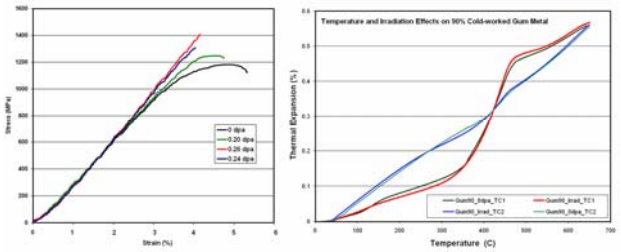

Figure 19: Effects of proton irradiation and temperature on stress-strain and thermal expansion of gum metal.

High-Z materials such as tantalum and tungsten were also irradiated to damage levels exceeding 1 dpa. The post-irradiation analysis revealed that the thermal expansion coefficient of tungsten is unaffected by irradiation, while the tantalum undergoes a phase transformation similar to that of super-invar and gum metal. Irradiation damage, while not affecting the thermal expansion coefficient of the material in the temperature range up to ~500°C, induces changes in the observed transition temperature.

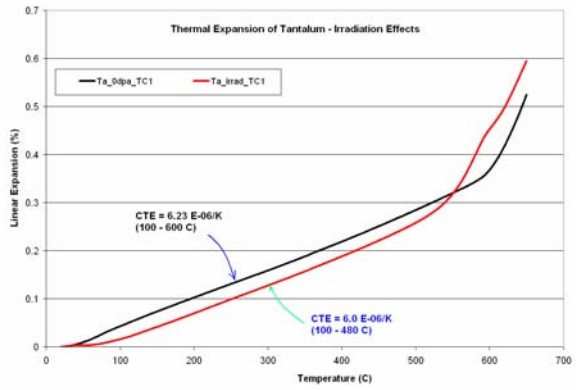

Figure 20: Effects of proton irradiation on the thermal expansion of tantalum.

DISCUSSION AND SUMMARY

This paper presents partial results of a comprehensive irradiation damage study of materials, alloys and composites considered for targets in multi-MW power future accelerators. The study aimed at evaluating the effects of high-energy protons on materials, in contrast to neutron irradiation and damage that has been studied extensively in nuclear reactors.

The continuing study has thus far revealed a number of intriguing points associated with how materials respond to proton irradiation. In particular,

- Carbon composites, characterized by low thermal expansion (even negative coefficient under quasi-static conditions up to about 800°C), experience dramatic change in the coefficient with the onset of irradiation.
- Thermal annealing fully restores the thermal expansion properties of carbon composites.
- Exceeding of a threshold in proton fluence (>5x10^{20} protons/cm^2) leads to severe structural degradation of carbon composites.
- Fine-grained isotropic graphite appears to be as vulnerable to high proton fluences as carbon composites.
- The observed susceptibility of graphite raises several questions. These stem from the fact that other types of graphite have survived much longer exposures under neutron irradiation without experiencing the kind of degradation observed. In an effort to explain the discrepancy the investigation is addressing (a) the damage potential of protons *vs.* neutrons, (b) the energy of the irradiating particles (high energy protons *vs.* thermal neutrons), (c) the rate of irradiation, and (d) the environment (water *vs.* inert gas even though irradiation temperatures remained below oxidation temperature in graphite).
- Interesting damage reversal through annealing was observed in super-Invar. The material, unlike other metals exhibiting irradiation defect removal, appears capable of restoring the thermal expansion property after subsequent irradiation exposures. Recent

irradiation with neutrons will help validate this very significant response of super-invar.

- Alloys such as “gum” metal that possess an optimal combination of physical and mechanical properties in its un-irradiated condition, appeared to be susceptible even to modest irradiation damage.
- The Vascomax alloy, while susceptible to corrosion, exhibits a remarkable ability of maintaining its ductility after irradiation

To help answer questions surrounding proton and neutron irradiation effects, a special arrangement at the BNL BLIP target station has allowed for the irradiation of target materials with neutrons characterized by energy spectra such as those shown in Fig. 6. The expectation is that following the post-irradiation analysis a damage correlation between protons and neutrons will emerge, which will allow high-power accelerator target studies to utilize the wealth of data associated with neutron irradiation.

REFERENCES

[1] N. Simos, et al., “Experimental studies of targets and collimators for high intensity beams,” Proceedings of HB2006, Paper No. TUBZ04, pp. 143-149, 2006.

[2] N. Simos, et al., “Solid Target Studies for Muon Colliders and Neutrino Beams,” Nucl. Phys. B (Proc. Suppl.) 155, 288-290 (2006).

[3] N. Simos, et al., “Target Material Irradiation Studies for High-Intensity Accelerator Beams,” Nucl. Phys. B (Proc. Suppl.) 149, 259-261 (2005).

[4] H.G. Kirk, et al., “Target Studies with BNL E951 at the AGS,” Proc. 2001 PAC, (Chicago, IL, March 2001), p.1535.

[5] N. Maruyama and M. Harayama, “Neutron irradiation effect on thermal conductivity and dimensional change of graphite materials,” Journal of Nuclear Materials, 195, 44-50 (1992).

[6] T. Saito, et al., Multifunctional Alloys Obtained via a Dislocation-Free Plastic Deformation Mechanism, Science, 300 (2003) 464

[7] Y. Ishiyama, et al., Journal of Nuclear Materials, 239 (1996) 90.

[8] N. Mokhov, “The MARS Code System User’s. 0 10 Guide”, Fermilab-FN-628 (1995)

[9] MCNPX Users Manual-Version 2.1.5, L.S. Waters, ed., LANL, Los Alamos, NM. TPO-E83-GUG-X-00001, (1999)